Characteristics of uphill diffusion with low frequency fluctuation in dipole magnetic field

N. Kenmochi[1], Y. Yokota[1], M. Nishiura[1,2], H. Saitoh[1], K. Nakamura[1], T. Mori[1], Z. Yoshida[1]

[1]*Graduate School of Frontier Sciences, The University of Tokyo, Kashiwa, Chiba, Japan*

[2]*National Institute of Fusion Science, Toki, Gifu, Japan*

Introduction

The Ring Trap 1 (RT-1) device is a laboratory magnetosphere that is realized by a levitated superconducting ring magnet in vacuum [1, 2]. The RT-1 experiment has demonstrated the self-organization of a plasma clump with a steep density gradient; a peaked density distribution is spontaneously created through 'uphill (inward) diffusion' [3, 4]. In the high-density regime of RT-1, interferometers and a reflectometer have observed edge localized fluctuations in the electron density which has a discrete spectrum of cascade modes at frequency less than 1 kHz. The fluctuation level increases obviously near the cut-off density, suggesting the density dependence of the fluctuations. The particle transport characterizes a turbulent diffusion driven by the electric-field fluctuations which are related to the presence of entropy modes observed in a laboratory magnetospheric plasma of the LDX [5, 6]. The underlying mechanism of the uphill diffusion is the adiabatic invariance of the magnetic moment, which puts a topological constraint on the diffusion process of particles across magnetic field lines [7]. The self-organized sharp density gradient is thought to be generated by the random walk of magnetized particles, driven by low-frequency fluctuations, which tends to homogenize the number of particles contained in each flux-tube. By perturbing the density profile by neutral-gas injection, we demonstrate the excitation of low-frequency fluctuations which persist until the uphill diffusion reproduces the self-organized density profile.

Experimental set-up

We studied the particle transport by investigating the time evolutions of electron density (n_e) profiles after the gas-puff injection. In a high-density plasma such as tokamak/helical devices, the injected neutrals are ionized in the peripheral region where the density are of 10^{18}~10^{19} m^{-3} and do not penetrate into the core region by the gas-puff injection. Therefore, they usually use the density modulation techniques to investigate the particle transport. On the other
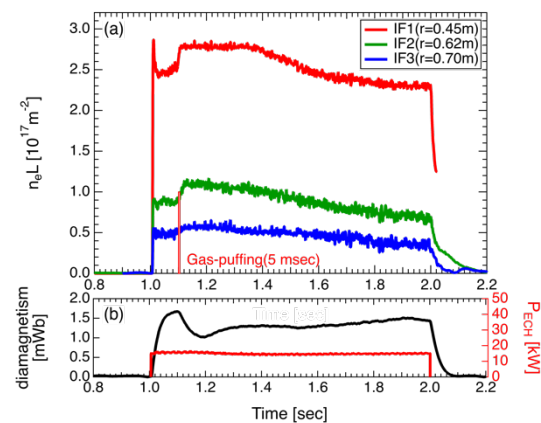

FIG. 1. Time evolution of (a) the line-integrated densities for the three chords of the interferometers and (b) that of the plasma stored energy and injection power of ECRH. The neutral gas was injected during 5 msec at t = 1.1 sec.

hand, in the RT-1, the neutrals can penetrate into the core region due to the low density of $10^{16} \sim 10^{17}$ m^{-3} in the edge region.

One shot of helium (He) gas was injected during 5 msec at $t = 1.1$ sec using a piezoelectric gas control valve. Figure 1 shows the time evolution of line-integrated electron density ($n_e L$), the plasma stored energy, and the injection power of electron cyclotron resonance heating (ECRH). The plasmas have been generated by using ECRH with 2.45 GHz microwaves from $t = 1.0$ to 2.0 sec. The $n_e L$ was measured by three 75 GHz ($\lambda = 4$ mm) heterodyne interferometers located at horizontal chord at $r = 0.45$ m and vertical chords at $r = 0.62$ and 0.70 m. The $n_e L$ measured by the horizontal chord of the interferometer at $r = 0.45$ m increases rapidly about 10 %, and starts decreasing at $t = 1.4$ s, whereas the densities of other two chords decrease just after the gas-puffing.

Formation of self-organized plasmas

For the spacial profile of density, the measured $n_e L$ is reconstructed by introducing a model function of magnetic flux surfaces [6, 7] which is given by

$$n_e(r,z) = n_0 \exp\left(-a\left(\frac{\psi(r,z) - \psi'}{\psi_0}\right)^2\right)\left(\frac{B(r,z)}{B_{z=0}}\right)^{-b}$$

Here, the parameters n_0, a and b are determined by fitting the measured $n_e L$. The term $\left(\frac{B(r,z)}{B_{z=0}}\right)^{-b}$ appears in this model to express the trapped orbits of the particles in a poloidal plane. The reconstructed density profiles at $t = 1.1$ sec and $t = 1.4$ sec are shown in FIG. 2(a) and (b). The subtraction of the latter profile from the former one is plotted in FIG. 2(c). The subtracted profile shows the time evolution of the electron transport. The spontaneous increase in density is clearly appeared at $r = 0.55$ m. The area differs from the fundamental harmonic ECR layers, where the plasma is produced. From the particle balance equation, He$^+$ is ionized within about 10 ms, and the density increases rapidly within 20 ms. The neutrals are supplied from the wall by the recycling particles uniformly, and not locally. Therefore, the spontaneous modification
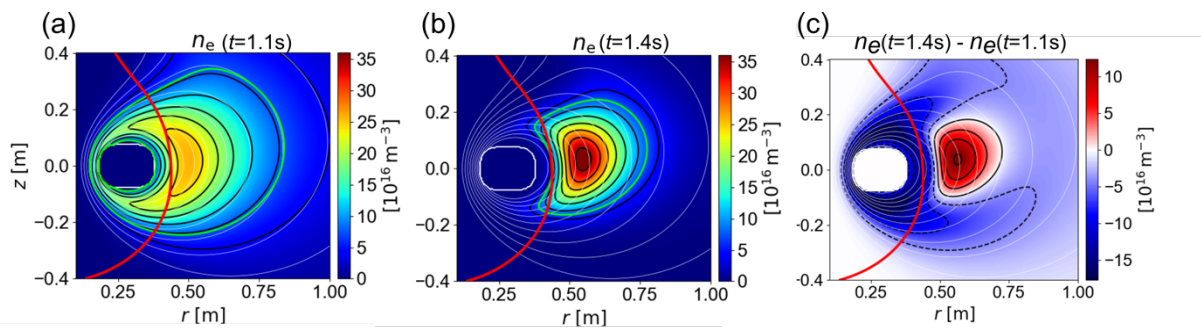

FIG. 2. The electron density profiles at (a) $t = 1.1$ s (just before the gas-puffing) and at (b) $t = 1.4$ s. (c) The subtracted profile of these two profiles. The reconstructed density profile at $t = 1.4$ s is subtracted from that at $t = 1.1$ s. The location for the fundamental harmonic resonances and cut-off density are indicated by the solid curves in red and green, respectively.

of the density profile is due to the uphill diffusion. This feature supports the fact that the heating beams with 2.45 GHz and 8.2 GHz produce the densities higher than the cut-off densities.

Characteristics of low-frequency fluctuation during uphill diffusion

Simultaneous excitation of low-frequency (~ 1 kHz) fluctuations during the uphill diffusion are observed in electrostatic potential, density, and magnetic field ($B_{\parallel}$ direction) measured by a floating potential probe, the interferometers, and magnetic probes, respectively. The fluctuations show a high coherence of above 0.6 between the density and magnetic measurements. The both three chords of interferometer and the 10 radial chords of He-line ratio-spectroscopy of the density-sensitive line ratio revealed that the fluctuations are localized in the peripheral region of the peaked density profile, which suggests the localized fluctuations drive the uphill diffusion. On the other hand, the fluctuation is not observed in the electron-temperature-sensitive line ratio for the He-line ratio-spectroscopy. As the pressure increases, (1) the amplitude of magnetic fluctuation increases with the threshold value of local electron beta (β_e) ~ 0.1, and (2) the frequency of the dominant fluctuation decreases in the region of β_e < 0.1 and becomes constant of ~ 1 kHz in the region of β_e > 0.1.

The spatiotemporal structure of the fluctuations was investigated by the magnetic proves in a toroidal (perpendicular to the magnetic field) and z-direction (parallel to the magnetic field) array. The typical phase velocities for the low-frequency fluctuation in toroidal and z-direction are 30 km/s ($k_{\perp}$ = 0.003 cm^{-1}, $k_{\perp}\rho_i$ ~ 0.02) and 2 km/s ($k_{\parallel}$ = 0.03 cm^{-1}, $k_{\parallel}\rho_i$ ~ 0.2), respectively. Here, the $k_{\perp}$ and $k_{\parallel}$ are wave number in the perpendicular and parallel direction to the magnetic field, respectively, and the ρ_i is ion gyroradius. The phase velocity in the z-direction increases from 1.5 km/s to 2.5 km/s as the increase of β_e (see FIG. 3(c)). The phase velocity in z-direction reversed directions when a limiter was inserted to z = - 0.15 m, r = 0.2 m from below the floating coil. This result suggests that the propagation of the fluctuations in z-direction are related to the mass flow which is considered to
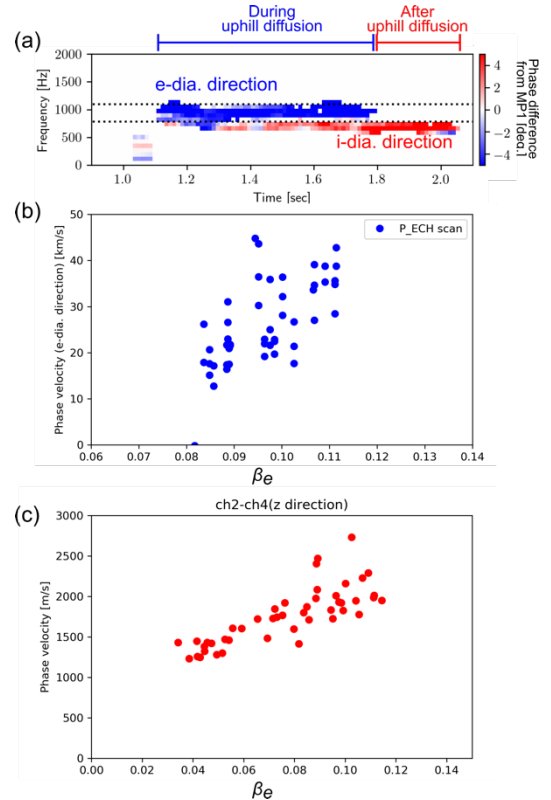

FIG. 3. (a) Time evolution of phase difference of two magnetic probes toroidally separated by $\Delta\varphi$ = 45 degrees. The β_e dependence of (b) the toroidal phase velocity in electron diamagnetic direction and (c) that of the phase velocity in z direction.

reverse the direction from +z to -z direction by the limiter. Figure 3(a) shows the time evolution of phase difference for each frequency between two magnetic probes toroidally separated by $\Delta\varphi = 45$ degrees. The fluctuations of two frequency component (~ 1 kHz and ~ 0.7 kHz) are observed. During the uphill diffusion from $t = 1.1$ sec to $t = 1.8$ sec, the fluctuation of ~ 1 kHz propagates toroidally in the electron diamagnetic direction. After the uphill diffusion, on the other hand, the fluctuation of ~ 1 kHz disappeared and the fluctuation of ~ 0.7 kHz which propagate in the ion diamagnetic direction is gradually excited. The phase velocity of the fluctuation during the uphill diffusion is the same order of diamagnetic drift velocity of 10^4 m/s and it increases from 20 km/s to 40 km/s as the increase of β_e (see FIG. 3(b)). The results that (1) the toroidal phase velocity is comparable to the drift velocity, (2) the fluctuations have low wave number of $k_\perp = 0.003$ cm^{-1} and $k_\parallel = 0.03$ cm^{-1}, and (3) the propagation direction depends on the density profiles, suggest that the drift wave instability is a possible candidate for the low-frequency fluctuation. Future studies will be conducted for the identification of the mode for understanding its excitation mechanism.

Summary

The dynamical formation on plasma profiles is studied in the dipole plasma confinement system using the neutral-gas puffing technique. After the neutral gas injection, the density with the peaked profile builds up associated with the electron density fluctuations in the frequency range of ~ 1 kHz. The electrons diffuse toward the higher density region to form the peaked density profile (uphill diffusion). The fluctuations are characterized as follows: (i) The amplitude and frequency depend on the plasma pressure. (ii) The excited fluctuation propagates toroidally in the electron diamagnetic direction from the onset of $t = 1.1$ sec. Another fluctuation in the ion diamagnetic direction is excited gradually in the frequency of 0.7 kHz. The fluctuation dominates at $t = 1.8$ sec, and then the density buildup due to uphill diffusion terminates. (iii) The phase velocity in the toroidal direction (~ 20 km/s) is comparable to the toroidal drift velocity. The phase velocity increases as the increase of plasma pressure.

References

[1] Z. Yoshida *et al.,* Plasma Fusion Res. **1** (2006) 008.

[2] Z. Yoshida *et al.,* Phys. Rev. Lett. **104** (2010) 235004

[3] M. Nishiura *et al*., Nucl. Fusion **55** (2015) 053019.

[4] M. Nishiura *et al*., Nucl. Fusion **57** (2017) 086038.

[5] A. C. Boxer *et al.*, Nature Phys. **6** (2010) 207.

[6] D. T. Garnier *et al*., Phys. Plasmas **24** (2017) 012506

[7] Z. Yoshida. Adv. Phys. X **1** (2016) 2.

[8] H. Saitoh *et al*., Phys. Plasmas **22** (2015) 024503.

[9] M. Nishiura *et al*., Nucl. Fusion, accepted manuscript online 2019.